Activation of H−H, C−H, C−C, and C−Cl Bonds by Pd(0). Insight from the Activation Strain Model

Axel Diefenbach[†,‡] and F. Matthias Bickelhaupt*[,§]

Fachbereich Chemie der Philipps-Universität Marburg, Hans-Meerwein-Strasse, D-35032 Marburg, Germany, and Afdeling Theoretische Chemie, Scheikundig Laboratorium der Vrije Universiteit, De Boelelaan 1083, NL-1081 HV Amsterdam, The Netherlands

Received: May 11, 2004; In Final Form: July 14, 2004

To achieve more insight into palladium-catalyzed H−H, C−H, C−C, and C−Cl bond activation and the mutual competition between these processes, several mechanistic pathways for oxidative addition of Pd(0) to H_2 (H−H), CH_4 (C−H), C_2H_6 (C−C and C−H), and CH_3Cl (C−Cl) were studied uniformly at the ZORA-BP86/TZ(2)P level of relativistic nonlocal density functional theory (DFT). Oxidative addition is overall exothermic for all model reactions studied, with 298 K reaction enthalpies ($\Delta H_{r,298}$) of −35.7 kcal/mol (C−Cl) through −9.7 kcal/mol (C−H in CH_4). The lowest barrier pathway is the direct oxidative insertion of Pd into the C−X or H−H bond (X = H, CH_3, Cl), with 298 K activation enthalpies ($\Delta H^{\ddagger}_{298}$) that increase in the order H−H (−21.7 kcal/mol) < C−Cl (−6.0 kcal/mol) ≈ C−H (−5.0 and −4.1 kcal/mol for CH_4 and C_2H_6) < C−C (9.6 kcal/mol). The "straight" S_N2 substitution resulting in $PdCH_3^+ + X^-$ or $PdH^+ + H^-$ is highly endothermic (144−237 kcal/mol) and thus not competitive. Only in the case of Pd + CH_3Cl is a third pathway found in which S_N2 substitution occurs in concert with a rearrangement of the Cl^- leaving group from C to Pd (S_N2/Cl-ra) leading, in one step, to CH_3PdCl via an activation barrier $\Delta H^{\ddagger}_{298}$ of 21.2 kcal/mol. The competition between the various bond activation processes is analyzed using the activation strain model in which activation energies ($\Delta E^{\ddagger}$) are decomposed into the activation strain ($\Delta E^{\ddagger}_{strain}$) of and the stabilizing transition state (TS) interaction ($\Delta E^{\ddagger}_{int}$) between the reactants in the activated complex: $\Delta E^{\ddagger} = \Delta E^{\ddagger}_{strain} + \Delta E^{\ddagger}_{int}$. Interestingly, the activation strain $\Delta E^{\ddagger}_{strain}$ adopts characteristic values for each type of bond and reaction mechanism. The trend in TS interaction $\Delta E^{\ddagger}_{int}$ turns out to be mainly determined by the donor−acceptor orbital interactions between occupied Pd 4d atomic orbitals and the empty σ^*_{C-X} (or σ^*_{H-H}) acceptor orbital associated with the bond to be activated in the substrate.

1. Introduction

Oxidative addition (eq 1) is a key step in many catalytic reactions[1] and has thus been intensively investigated both experimentally[2−7] and theoretically.[5,7−12]

$$ML_n + R{-}X \underset{\text{reductive elimination}}{\overset{\text{oxidative addition}}{\rightleftharpoons}} R{-}ML_n{-}X \qquad (1)$$

The aim of this investigation is to obtain a better understanding of how the electronic structure of a catalyst determines its reactivity toward the archetypical H−H, C−H, C−C, and C−Cl bonds in H_2, CH_4, C_2H_6, and CH_3Cl. This is of interest also for industrial chemistry, because it enables a more rational design of catalytically active species. One example is the activation and subsequent functionalization of the rather inert alkanes (e.g., CH_4).[13a] Whereas the long-term purpose of our efforts is understanding and directing, in a rational manner, the factors that determine the catalytic activity and selectivity of transition metal *complexes*, the starting point is the investigation of the *intrinsic* reactivity of the transition metal *atom*. Thus, by introducing ligands in a second stage, it can be precisely assessed how they interfere with the metal electronic structure and how they exactly affect the activity and selectivity of the resulting homogeneous catalyst. This modular approach to theoretical homogeneous catalysis is designated fragment-oriented design of catalysts (FDC).

In the present work, a detailed study of the *intrinsic* reactivity of the uncoordinated Pd(0) atom toward H_2, CH_4, C_2H_6, and CH_3Cl has been carried out using relativistic nonlocal density functional theory (DFT) at the ZORA-BP86/TZ(2)P level (see section 2). This approach was shown previously to yield reliable trends in reactivity for oxidative insertion of Pd into the C−H, C−C, and C−Cl bonds of methane, ethane, and chloromethane.[14] Palladium was chosen because this metal is widely used in catalysis[13] and because the atom has a stable closed-shell d^{10} ground state,[8a,12b] which facilitates comparison with closed-shell Pd(0) complexes in future investigations. Thus, we have explored the potential energy surfaces (PES) of the following model reactions (eq 2):

$$\text{H−H activation:}\quad Pd + H_2 \rightarrow H{-}Pd{-}H \qquad (2)$$

$$\text{C−H activation:}\quad Pd + CH_4 \rightarrow CH_3{-}Pd{-}H \qquad (2b)$$

$$Pd + C_2H_6 \rightarrow CH_3CH_2{-}Pd{-}H \qquad (2c)$$

$$\text{C−C activation:}\quad Pd + C_2H_6 \rightarrow CH_3{-}Pd{-}CH_3 \qquad (2d)$$

$$\text{C−Cl activation:}\quad Pd + CH_3Cl \rightarrow CH_3{-}Pd{-}Cl \qquad (2e)$$

For each of the five model reactions of eq 2, the direct oxidative insertion (OxIn) mechanism (eq 3a) and an alternative

* Corresponding author. Fax: +31-20-44 47629. E-mail: FM.Bickelhaupt@few.vu.nl.
† Fachbereich Chemie der Philipps-Universität Marburg.
‡ Present address: Sercon GmbH.
§ Scheikundig Laboratorium der Vrije Universiteit.

10.1021/jp047986+ CCC: $27.50
Published on Web 09/14/2004

S_N2 type reaction that overall leads also to oxidative addition (eq 3b) is studied.

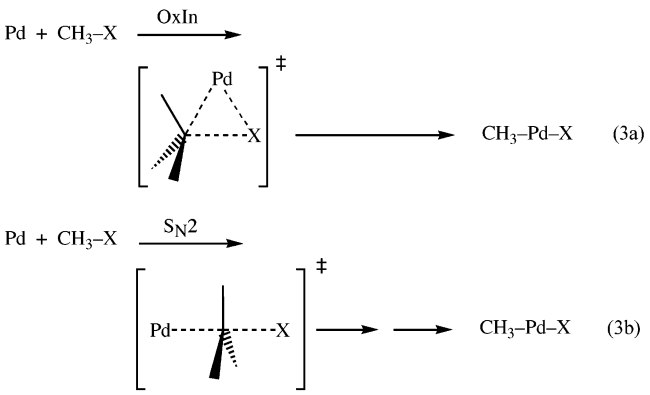

This extends our previous work in three ways: (i) the H−H bond is included; (ii) the C−H bond is now studied in two different substrates, methane and ethane; and (iii) for all bonds an S_N2 pathway is included into the exploration of the PES, in addition to direct oxidative insertion. In this way, a uniform treatment of different reaction mechanisms for the broad spectrum of H−H, C−H, C−C, and C−Cl bond activation is achieved.

The competition between the various bond activation processes and mechanisms is analyzed using the activation strain (or activation strain−TS interaction, ATS) model originally introduced in the context of elementary organic reactions.[10a] In the activation strain model, activation energies ($\Delta E^{\ddagger}$) are decomposed into the activation strain ($\Delta E^{\ddagger}_{\text{strain}}$) of and th stabilizing transition state (TS) interaction ($\Delta E^{\ddagger}_{\text{int}}$) between the reactants in the activated complex: $\Delta E^{\ddagger} = \Delta E^{\ddagger}_{\text{strain}} + \Delta E^{\ddagger}_{\text{int}}$. At this point, we anticipate that the activation strain $\Delta E^{\ddagger}_{\text{strain}}$ turns out to adopt characteristic values for each type of bond and reaction mechanism. Furthermore, the concept of TS interaction $\Delta E^{\ddagger}_{\text{int}}$ provides the necessary basis for understanding how the activity of a catalyst depends on its electronic structure.

This paper is organized as follows. After the description of our quantum chemical method in section 2, we proceed in section 3.1 with the exploration of the PES of the various model reactions. Next, in section 3.2, the activation strain model of chemical reactivity is introduced. This model is applied in section 3.3 in which the competition between the different model bond activation processes, i.e., the relative heights of activation barriers, is analyzed. The conclusions are summarized in section 4.

2. Methods

All calculations are based on density functional theory (DFT)[15,16] and have been performed using the Amsterdam density functional (ADF) program.[17] MOs were expanded in a large uncontracted set of Slater-type orbitals (STOs).[17h] The basis is of triple-ζ quality, augmented with two sets of polarization functions: 2p and 3d for hydrogen and 3d and 4f for carbon, oxygen, and chlorine. The palladium atom is represented by a triple-ζ type basis set augmented with one 5p polarization function. The core shells of carbon (1s), oxygen (1s), chlorine (1s2s2p), and palladium (1s2s2p3s3p3d) were treated by the frozen-core approximation.[17b] An auxiliary set of s, p, d, f, and g STOs was used to fit the molecular density and to represent the Coulomb and exchange potentials accurately in each SCF cycle.[17i]

Geometries and energies were calculated using the generalized gradient approximation (GGA). Exchange is described by Slater's Xα potential,[17j] with nonlocal corrections due to Becke.[17k,l] Correlation is treated in the Vosko−Wilk−Nusair (VWN) parametrization using formula V,[17m] with nonlocal corrections due to Perdew.[17n] Relativistic effects were taken into account by the zeroth-order regular approximation (ZORA).[18] Prior investigations showed that relativistic effects are significant for our systems and that the ZORA formalism is well-suited for describing them.[14]

All energy minima and transition state[17r] structures were verified by frequency calculations:[17q] for minima all normal modes have real frequencies, whereas transition states have one normal mode with an imaginary frequency. The character of the normal mode associated with the imaginary frequency was analyzed to ensure that the correct transition state was found.

Enthalpies at 298.15 K and 1 atm (ΔH_{298}) were calculated from 0 K electronic energies (ΔE) according to eq 4, assuming an ideal gas.[19]

$$\Delta H_{298} = \Delta E + \Delta E_{\text{trans},298} + \Delta E_{\text{rot},298} + \Delta E_{\text{vib},0} + \Delta(\Delta E_{\text{vib},0})_{298} + \Delta(pV) \quad (4)$$

Here, $\Delta E_{\text{trans},298}$, $\Delta E_{\text{rot},298}$, and $\Delta E_{\text{vib},0}$ are the differences between products and reactants in translational, rotational, and zero point vibrational energy, respectively; $\Delta(\Delta E_{\text{vib}})_{298}$ is the change in the vibrational energy difference as one goes from 0 to 298.15 K. The vibrational energy corrections are based on the frequency calculations. The molar work term $\Delta(pV)$ is $(\Delta n)RT$; $\Delta n = -1$ for two reactants (e.g., Pd and CH_3X) combining to one species. Thermal corrections for the electronic energy are neglected.

3. Results and Discussion

3.1. Reaction Profiles and Geometries. In this section, the potential energy surfaces (PES) of the various oxidative insertion and S_N2 reactions are discussed. The results are summarized in Figures 1 and 2 (geometries) and Table 1 (energies). First, the direct oxidative insertion (OxIn) reactions are presented. For all substrates, they proceed from a reactant complex via a TS to a product; see Figure 1.

The oxidative insertion of Pd + H_2 comes along with a relatively flat PES; see Table 1. The activation barrier is −21.7 kcal/mol[20] relative to the reactants. In the transition state, the H−H bond distance has been stretched by 0.634 Å (85%) and amounts to 1.383 Å. There is essentially no reverse barrier, only a slight barrier of 0.5 kcal/mol on the electronic energy surface.

The C−H activation is investigated using two different substrates, CH_4 (**2a**) and C_2H_6 (**3a**). In this way, we can reveal if, for example, the activation strain (see section 3.2) adopts a characteristic value for a particular type of bond (i.e., the C−H bond) in different substrates. Geometries for both reactions are shown in Figure 1 (structures **2a**−**d** and **3a**−**d**). Again, one finds relatively stable reactant complexes, **2b** and **3b**, respectively, in which Pd binds symmetrically to two C−H bonds of the substrate. Such a high stability is confirmed by gas-phase experiments where corresponding long-range complexes could be found for some alkanes.[7b] In fact, the reactant complexes for all substrates but CH_3Cl are of about the same thermodynamic stability as the corresponding product of oxidative addition to Pd. For CH_4 (eq 2b), the activation enthalpy is −5.0 kcal/mol relative to the reactants. In the TS, the C−H bond has been stretched by 0.517 Å (47%) and amounts to 1.613 Å. The C−H activation in C_2H_6 (eq 2c) proceeds via a transition state **3c** at −4.1 kcal/mol relative to the reactants, to a product **3d** at

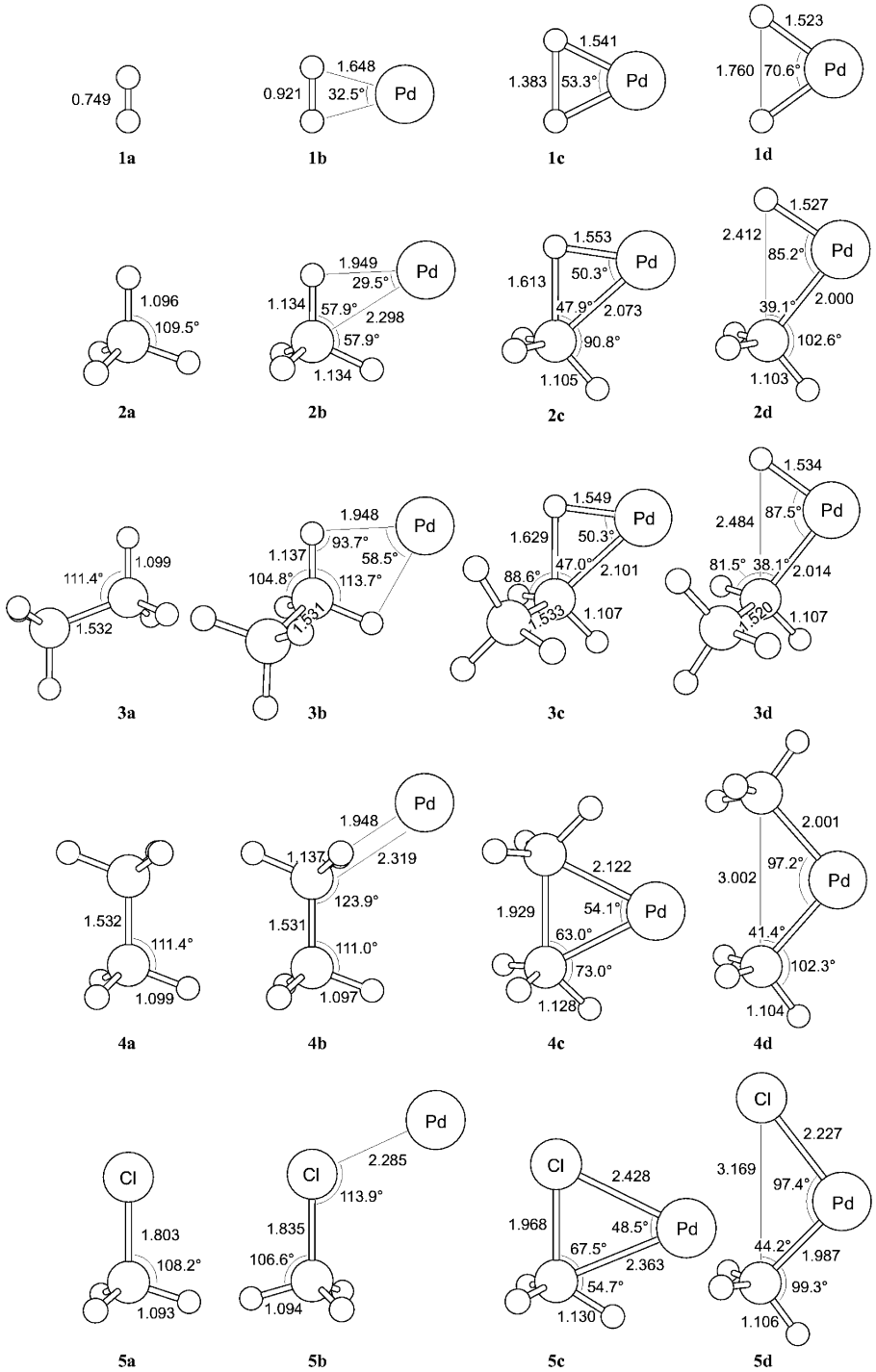

Figure 1. Geometries (in Å, deg) at ZORA-BP86/TZ(2)P of stationary points along the potential energy surface for oxidative insertion (OxIn) reaction of Pd into the H−H bond of H_2 (**1**), the C−H bond of CH_4 (**2**), the C−H bond of C_2H_6 (**3**), the C−C bond of C_2H_6 (**4**), and the C−Cl bond of CH_3Cl (**5**).

−11.6 kcal/mol. The C−H bond of the TS is lengthened by 0.530 Å (48%) and amounts to 1.629 Å. This is very similar to the C−H activation of CH_4. The reaction may further proceed via a second transition state (0.6 kcal/mol above **3d** and corresponding to an internal rotation around the Pd−C bond) to a conformation that is 0.4 kcal/mol more stable than the initial product complex **3d**.

The OxIn activation of the C−C bond of ethane (eq 2d) starts from the reactant complex **4b** being identical to structure **3b**. The barrier of the transition state **4c** is 9.6 kcal/mol, significantly higher than in the H−H or C−H activation. Yet, in the TS, the C−C bond is only stretched by 0.397 Å (26%) and amounts to 1.929 Å; the relative stretching is less than in the H−H and C−H activations.

The activation of CH_3Cl **5a** by direct oxidative insertion of Pd is connected with a slight lengthening of the C−Cl bond by 0.165 Å (9%) in the TS, where this bond has a length of 1.968 Å. The activation barrier of −6.0 kcal/mol is lower than for the C−H and C−C activation. The formation of product **5d** is the most exothermic oxidative addition among the model reactions studied, with a reaction enthalpy of −35.7 kcal/mol.

The activation enthalpies $\Delta H^{\ddagger}_{298}$ increase in the order H−H < C−Cl ≤ C−H < C−C. Previous explanations concentrate on the directionality of the methyl sp^3 orbital[11n] and on the

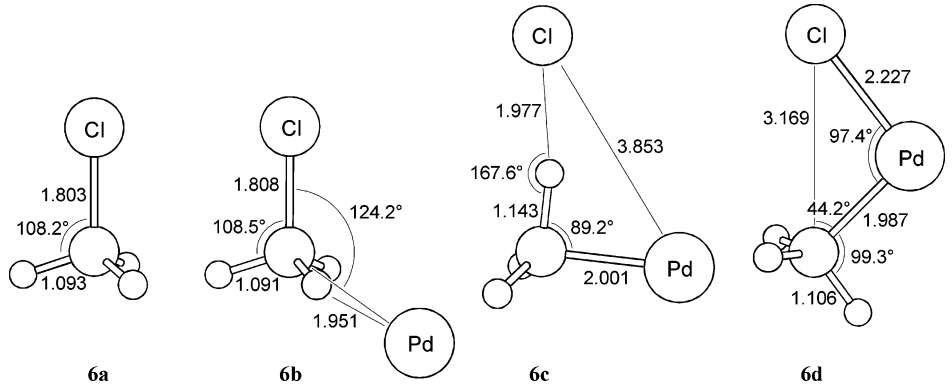

Figure 2. Geometries (in Å, deg) at ZORA-BP86/TZ(2)P of stationary points along the potential energy surface for the S_N2/Cl-rearrangement reaction of Pd with CH_3Cl.

TABLE 1: Reaction Profiles at BP86/TZ(2)P for the Oxidative Insertion, the S_N2, and the S_N2/Leaving Group Rearrangement Reactions of Pd with H_2, CH_4, C_2H_6, and CH_3Cl: 298 K Enthalpies (in kcal/mol) Relative to the Reactants

activated bond	reactants	reactant complex	transition state	product
		Oxidative Insertion		
H−H	Pd + H_2	−24.4	−21.7	−21.1
		(−24.1[a])	(−21.7[a])	(−22.2[a])
C−H	Pd + CH_4	−11.4	−5.0	−9.7
	Pd + C_2H_6	−11.6	−4.1	−11.6[b]
C−C	Pd + C_2H_6	−11.6	9.6	−14.1
C−Cl	Pd + CH_3Cl	−15.6	−6.0	−35.7
		S_N2 Substitution		
H−H	Pd + H_2	−24.4	d	237.0[e]
C−H	Pd + CH_4	−11.4	d	228.7[e]
C−C	Pd + C_2H_6	−11.6	d	228.6[e]
C−Cl	Pd + CH_3Cl	−10.1[c]	d	143.5[e]
		S_N2/Cl-Rearrangement		
C−Cl	Pd + CH_3Cl	−10.1	21.2	−35.7

[a] Zero Kelvin electronic energies. [b] Primary product of insertion. Rearrangement via second TS (−11.0 kcal/mol) to final product (−12.0 kcal/mol). [c] Separate S_N2 reactant complex: Pd coordinates symmetrically to two C−H bonds of chloromethane. [d] No reverse activation barrier. [e] Dissociated products of straight S_N2 reaction.

energy necessary to tilt the methyl groups of CH_4 and C_2H_6 toward the metal:[11i] in C_2H_6, there are two methyl groups to be bent, which leads to a higher barrier. However, as will become clear in section 3.3, the activation strain analysis reveals that it is not a higher strain in ethane that causes the barrier for C−C activation to be higher than that of C−H activation.

Next, the S_N2 type reactions are discussed. The products of the "straight" S_N2 reaction, i.e., $PdH^+ + H^-$ and $PdCH_3^+ + H^-$, CH_3^- and Cl^-, are highly endothermic due to the concomitant charge separation, with reaction enthalpies ranging from 144−237 kcal/mol (Table 1).[22] All S_N2-type reactions occur without reverse activation barrier. In other words, there is no stationary point on the PES associated with a regular S_N2 transition state. However, for reaction 2e, Pd + CH_3Cl, a transition state, **6c**, could be found that corresponds to an S_N2 substitution occurring in concert with a rearrangement of the leaving group Cl^- (S_N2/Cl-ra); see Figure 2. This leads to the oxidative addition product **6d**. The latter is identical to structure **5d**. Note, however, that the S_N2/Cl-ra mechanism goes with inversion of configuration at the carbon atom of the activated C−X bond, whereas the OxIn mechanism is associated with retention of configuration. Thus, the two pathways yield different enantiomers as product in the case of more complex substrates that involve an asymmetric carbon atom in the activated C−X bond. In forthcoming studies, using the activation strain model, we aim at rationally tuning the relative reactivity of these two pathways and, thus, the stereochemistry of C−Cl bond activation. For the other substrates, a TS associated with an S_N2/Cl-ra mechanism could not be found. The barrier of the S_N2/Cl-ra pathway of Pd + CH_3Cl, although much lower than that for straight S_N2 substitution, is 21.2 kcal/mol, still much higher than the barrier of direct oxidative insertion (−6.0 kcal/mol, Table 1).[22]

Entropy effects at 298 K are important in the sense that they increase the magnitude of the activation free energy $\Delta G^{\ddagger}$ by a few kcal/mol, but they do not discriminate much between the various bond activation reactions and pathways considered. Thus, the 298 K activation entropies $\Delta S^{\ddagger}$ for direct oxidative insertion (OxIn) of Pd are all negative and amount to −18.1 (H−H), −22.5 (C−H in methane), −24.3 (C−H in ethane), −26.1 (C−C), and −23.4 cal/mol K (C−Cl); the activation entropy for the S_N2/Cl-ra pathway to C−Cl bond activation is −21.6 kcal/mol (entropies are not shown in Table 1). The corresponding $-T\Delta S^{\ddagger}$ values vary from 5.4 (H−H) to 7.8 (C−C) kcal/mol, which, in terms of relative activation free energies $\Delta G^{\ddagger}$, essentially does not change the picture that arises from the activation energies $\Delta E^{\ddagger}$. Therefore, in the following, we focus on further analyzing the origin of and difference between the energy barriers $\Delta E^{\ddagger}$ of the reactions.

3.2. Activation Strain Model. To gain insight into how the activation barriers of the different oxidative insertion reactions arise, i.e., insight into how they depend on the nature of the concomitant geometrical deformation and electronic structure of catalyst and substrate, they were analyzed using the activation strain model of chemical reactivity.[10a] In this model, the activation energy $\Delta E^{\ddagger}$ is decomposed into the activation strain $\Delta E^{\ddagger}_{\text{strain}}$ and the transition state (TS) interaction $\Delta E^{\ddagger}_{\text{int}}$ (see eq 5 and Figure 3):

$$\Delta E^{\ddagger} = \Delta E^{\ddagger}_{\text{strain}} + \Delta E^{\ddagger}_{\text{int}} \tag{5}$$

The activation strain $\Delta E^{\ddagger}_{\text{strain}}$ is the strain energy associated with deforming the reactants from their equilibrium geometry to the geometry they acquire in the activated complex (Figure 3). The TS interaction $\Delta E^{\ddagger}_{\text{int}}$ is the actual interaction energy between the deformed reactants in the transition state. In the present study, one of the reactants is the Pd-d^{10} atom and the other reactant is one of the substrates H_2, CH_4, C_2H_6, and CH_3Cl.

The TS interaction $\Delta E^{\ddagger}_{\text{int}}$ between the strained reactants is further analyzed in the conceptual framework provided by the Kohn−Sham molecular orbital (KS-MO) model.[16] To this end, it is further decomposed into three physically meaningful terms

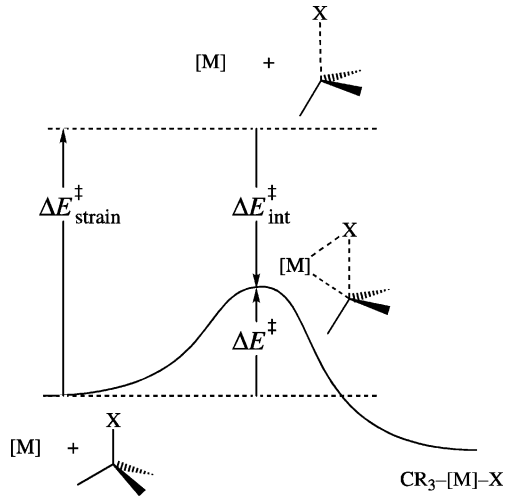

Figure 3. Illustration of the activation strain model in case of C−X bond activation by a transition metal system [M]. The activation energy $\Delta E^{\ddagger}$ is decomposed into the activation strain $\Delta E^{\ddagger}_{strain}$ of and the stabilizing TS interaction $\Delta E^{\ddagger}_{int}$ between the reactants in the transition state ($\Delta E^{\ddagger}_{int}$ may be further analyzed).

TABLE 2: Analysis of the Activation Energies for Oxidative Insertion of Pd into the Indicated Bonds of H_2, CH_4, C_2H_6, and CH_3Cl in Terms of the Activation Strain Model

activated bond	H_2 H−H	CH_4 C−H	C_2H_6 C−H	C_2H_6 C−C	CH_3Cl C−C1
Energy Decomposition (in kcal/mol)					
$\Delta E^{\ddagger}$	−21.7	−1.6	−0.7	12.6	−4.3
$\Delta E^{\ddagger}_{strain}$	55.6	53.5	54.7	39.4	8.8
$\Delta E^{\ddagger}_{int}$	−77.3	−55.1	−55.4	−26.8	−13.1
ΔE_{Pauli}	208.7	211.1	209.8	192.6	112.3
ΔV_{elst}	−183.7	−170.4	−171.9	−139.5	−76.7
ΔE_{oi}	−102.3	−95.8	−93.3	−79.9	−48.7
Fragment Orbital Overlap ⟨Pd|substrate⟩					
⟨4d|LUMO⟩	0.300	0.327	0.450	0.136	0.082
⟨5s|HOMO⟩	0.566	0.401	0.359	0.213	0.144
Fragment Orbital Population (in electrons)					
Pd 5s	0.45	0.38	0.38	0.22	0.18
Pd 4d	9.28	9.32	9.31	9.42	9.59
substrate LUMO	0.43	0.36	0.36	0.25	0.17
substrate HOMO	1.73	1.71	1.74	1.83	1.91
Fragment Orbital Energy (in eV)					
Pd 5s	−3.423	−3.423	−3.423	−3.423	−3.423
Pd 4d	−4.193	−4.193	−4.193	−4.193	−4.193
substrate LUMO	−2.854	−1.625	−1.597	−0.391	−2.066
substrate HOMO	−8.438	−7.435	−6.806	−7.303	−7.142

(eq 6) using the extended transition state (ETS) method[21] developed by Ziegler and Rauk.

$$\Delta E^{\ddagger}_{int} = \Delta V_{elst} + \Delta E_{Pauli} + \Delta E_{oi} \qquad (6)$$

The term ΔV_{elst} corresponds to the classical electrostatic interaction between the unperturbed charge distributions of the deformed reactants and is usually attractive. The Pauli repulsion (ΔE_{Pauli}) comprises the destabilizing interactions between occupied orbitals and is responsible for the steric repulsion. The orbital interaction (ΔE_{oi}) accounts for charge transfer (interaction between occupied orbitals on one moiety with unoccupied orbitals of the other, including the HOMO−LUMO interactions) and polarization (empty−occupied orbital mixing on one fragment due to the presence of another fragment).

3.3. Analysis of the Activation Barriers for Bond Activation. The results of the activation strain analysis are listed in Table 2. The activation energy $\Delta E^{\ddagger}$ takes, not unexpectedly, characteristic values for particular bonds and mechanisms. Thus, it differs for different bond types (e.g., C−H vs C−C) and mechanistic pathways (e.g., OxIn vs S_N2/Cl-ra), whereas it adopts more or less the same value for one type of bond, say an aliphatic C−H bond, in different substrates (for example, the C−H activation in CH_4, C_2H_6, and, not shown here, CH_3-Cl). This is true also for the activation strain $\Delta E^{\ddagger}_{strain}$. The latter adopts characteristic values for each type of bond. For example, for the palladium-induced activation of C−H and C−C bonds, it amounts to ca. 54 and 39 kcal/mol, respectively. However, an important difference between activation energy and activation strain is that the latter correlates neatly with the bond strength of the activated bond and with the percentage-wise extent of bond stretching in the transition state.[23] Typical strengths and lengths of the bonds under investigation are given: 104 (H−H), 99 (C−H), 83 (C−C), and 78 kcal/mol (C−Cl), and ∼0.7 (H−H), ∼1.1 (C−H), ∼1.5 (C−C), and ∼1.8 Å (C−Cl).[24] We recall that the relative bond stretching in the TS for oxidative insertion is 85% (H−H), ca. 47% (C−H), 26% (C−C), and 9% (C−Cl). Thus, both the bond strength and the percentage-wise bond elongation in the TS decrease in the order H−H > C−H > C−C > C−Cl. Note that the activation strain for direct insertion (OxIn) decreases in the same order, namely, from 56 to 54 to 39 to 9 kcal/mol along H−H, C−H, C−C, and C−Cl. Note in particular that the strain in the TS for C−C activation (39 kcal/mol) is lower than that for C−H activation (54 kcal/mol). This contradicts earlier explanations[11i,n] that ascribe the higher barrier for C−C than C−H activation to the higher strain that results from tilting the sp^3 hybridized SOMO of two instead of only one methyl group in the TS (see section 3.1). While it is obviously true that C−C activation involves tilting twice the number of methyl groups as C−H activation, it is simply not the decisive factor. The trend in activation strain is determined by the lesser extent (both absolute and percentage-wise) of C−C bond elongation that is required for achieving the TS for oxidative insertion of the Pd atom into this bond.

Whereas the activation strain $\Delta E^{\ddagger}_{strain}$ appears to depend in a straightforward manner on the strength and length of the activated bond,[23] no such obvious correlation exists for the activation barrier $\Delta E^{\ddagger}$, which shows a more complex behavior. This is because of the interplay of counteracting trends in $\Delta E^{\ddagger}_{strain}$ and $\Delta E^{\ddagger}_{int}$. The latter weakens from −77 to −55 to −27 to −13 kcal/mol along H−H, C−H, C−C, and C−Cl (see Table 2). To trace the origin of the trend in TS interaction, we have decomposed $\Delta E^{\ddagger}_{int}$ into electrostatic attraction ΔV_{elst}, Pauli repulsion ΔE_{Pauli}, and orbital interactions ΔE_{oi} between palladium and the substrate (see section 3.2). Both, the electrostatic attraction and Pauli repulsion correlate perfectly with the catalyst−substrate distance: they become weaker as the catalyst−substrate distance increases, i.e., in the order H−H > C−H > C−C > C−Cl, because of the decreasing overlap integrals (not shown in Table 2) between the charge density distributions/occupied orbitals of the two molecular fragments. The decrease in Pauli *repulsion* counteracts the overall trend in decreasing TS interaction. It is the orbital interaction energy ΔE_{oi} that together with the electrostatic attraction (vide supra) determines the trend in TS interaction: just as the latter, ΔE_{oi} become less stabilizing along the series H−H > C−H > C−C > C−Cl; see Table 2. The energy term ΔE_{oi} is provided by donor−acceptor interactions of the occupied orbitals of one fragment with the unoccupied orbitals of the other fragment (and vice versa) and tightly depends on orbital overlap properties and orbital energies of both the catalyst and the substrate frontier orbitals.

The Kohn−Sham MO analyses reveal two important orbital interaction features in the transition states **1c**, **2c**, **3c**, **4c**, and

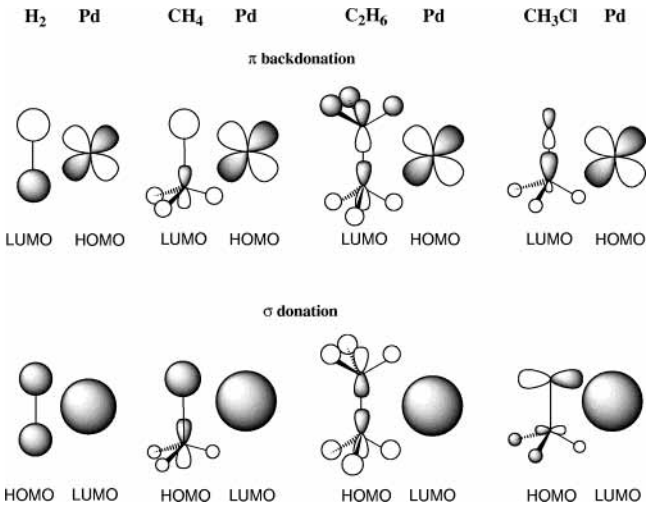

Figure 4. Schematic representation of the frontier orbital interactions between Pd and the substrates H_2, CH_4, C_2H_6, and CH_3Cl in the transition states for oxidative insertion, emerging from the Kohn−Sham MO analyses of the corresponding TS interactions $\Delta E^{\ddagger}_{int}$ at ZORA-BP86/TZ(2)P.

5c, which are shown in Figure 4: (i) back-donation from the Pd 4d atomic orbital (AO) into the substrate's LUMO (lowest unoccupied molecular orbital) and (ii) donation of the substrate's HOMO (highest occupied molecular orbital) into the Pd 5s AO. The Pd 5p orbitals do not significantly participate in these interactions. Back-donation from Pd 4d into the substrate's σ^* LUMO dominates the trend in ΔE_{oi} because of the relatively small orbital energy gap for this interaction. We recall that the stabilization ($\Delta\epsilon$) of the bonding Pd 4d + σ^* combination of fragment orbitals with respect to the energy of the occupied fragment orbitals [ϵ(Pd 4d)] is in good approximation proportional to $\langle \text{Pd 4d}|\sigma^*\rangle^2/\epsilon(\text{Pd 4d}) - \epsilon(\sigma^*)$, that is, the overlap integral squared divided by the difference in orbital energies.[25] As can be seen in Table 2, the HOMO−LUMO gap for back-donation, $\epsilon(\text{Pd 4d}) - \epsilon(\sigma^*)$, ranges from 1.3 to 3.8 eV and is thus significantly smaller than that for donation from the substrate HOMO to Pd 5s, which ranges from 3.7 to 5.0 eV. This makes Pd 4d−σ^* back-donation a stronger interaction with stronger relative variations and thus the dominant factor, while the influence of donation from the substrate HOMO into the Pd 5s LUMO is limited. The orbital energy difference $\epsilon(\text{Pd 4d}) - \epsilon(\sigma^*)$ increases significantly from 1.3 to 2.6 to 3.8 eV along H−H, C−H (both in methane and ethane), and C−C, in line with the trend of a decreasing overall ΔE_{oi} term (Table 2). The increasing HOMO−LUMO gap is caused by the fact that the extent of bond stretching in the transition state decreases (and thus the antibonding character of the substrate σ^* MO *increases*) along H−H, C−H, and C−C. Note that the orbital interactions continue to become weaker from C−C to C−Cl, whereas, in this step, the HOMO−LUMO gap $\epsilon(\text{Pd 4d}) - \epsilon(\text{substrate } \sigma^*)$ does *not* further increase. Instead, it decreases from 3.8 to 2.1 eV and is thus not responsible for the weakening of ΔE_{oi} along C−C and C−Cl. The decisive factor for this behavior of ΔE_{oi} is the continuing reduction of the $\langle \text{Pd 4d}|\sigma^*\rangle$ overlap along C−C to C−Cl from 0.14 to 0.08, the smallest overlap value for the whole series (see Table 2). The weakening in back-donation from Pd 4d to substrate σ^* along H−H, C−H, C−C, and C−Cl is also reflected by the fact that the extent of depopulation of the Pd 4d AOs decreases from 0.82 (H−H) to ca. 0.69 (C−H to 0.58 (C−C) to 0.41 electrons (C−Cl) along this series [i.e., the Pd 4d population increases from 9.28 (H−H) to ca. 9.31 (C−H) to 9.42 (C−C) to 9.59 electrons (C−Cl); see Table 2]. Fragment orbital populations also indicate that the trend in back-donation is further reinforced by that in (the energetically less important, vide supra) donation from substrate HOMO to Pd 5s; that is, the extent of depopulation of the substrate HOMO changes at first only slightly from 0.27 (H−H) to 0.26−0.29 (C−H) and then more pronouncedly to 0.17 (C−C) and 0.09 electrons (C−Cl) [i.e., the substrate HOMO population varies from 1.73 (H−H) to 1.71−1.74 (C−H) and increases thereafter more pronouncedly to 1.83 (C−C) and finally 1.91 electrons (C−Cl); see Table 2].

4. Conclusions

Pd(0)-catalyzed activation of prototypical H−H, C−H, C−C, and C−Cl bonds (i.e., oxidative addition of these bonds to a Pd d^{10} atom) is exothermic and occurs via direct oxidative insertion of the metal atom; an alternative nucleophilic substitution mechanism is kinetically strongly disfavored. Activation enthalpies $\Delta H^{\ddagger}_{298}$ for the OxIn pathway, computed at ZORA-BP86/TZ2P, increase in the order H−H < C−Cl ≈ C−H < C−C. To arrive at an understanding of the origin and relative heights of the reaction barriers associated with the above bond activation processes, we have analyzed them using the activation strain model in which the activation energy $\Delta E^{\ddagger}$ is decomposed into the activation strain $\Delta E^{\ddagger}_{strain}$ of and the stabilizing transition state (TS) interaction $\Delta E^{\ddagger}_{int}$ between the reactants in the activated complex: $\Delta E^{\ddagger} = \Delta E^{\ddagger}_{strain} + \Delta E^{\ddagger}_{int}$. Interestingly, the activation strain $\Delta E^{\ddagger}_{strain}$ adopts a characteristic value for a particular type of bond and reaction mechanism. In forthcoming work, we explore the possibility of using this concept for rationally steering the selectivity of a model catalyst. In a first stage, we aim at controlling the stereochemistry of C*−Cl bond activation (i.e. a C−Cl bond with an asymmetric carbon atom) by tuning, through a clever choice of one or more ligands, the TS interaction $\Delta E^{\ddagger}_{int}$ in favor of direct insertion (which leads to retention of configuration) or nucleophilic substitution (which leads to inversion of configuration).

Acknowledgment. We thank the Fonds der Chemischen Industrie (FCI) for a doctoral stipendium for A.D. and The Netherlands Organization for Scientific Research (NWO-CW) for financial support. We thank G. Theodoor de Jong for helpful discussions.

References and Notes

(1) (a) Collman, J. P.; Hegedus, L. S.; Norton, J. R.; Finke, R. G. *Principles and Applications of Organotransition Metal Chemistry*; University Science Books: Mill Valley, CA, 1987. (b) Elschenbroich, Ch.; Salzer, A. *Organometallics. A Concise Indroduction*, 2nd ed.; VCH: Weinheim, Germany, 1992. (c) Ritleng, V.; Sirlin, C.; Pfeffer, M. *Chem. Rev.* **2002**, *102*, 1731.

(2) Experimental studies on reactions of metal complexes in the condensed phase: (a) Luh, T.-Y.; Leung, M.-k.; Wong, K.-T. *Chem. Rev.* **2000**, *100*, 3187. (b) Stürmer, R. *Angew. Chem.* **1999**, *111*, 3509. (c) Hau, L.-B.; Tanaka, M. *Chem. Commun.* **1999**, *5*, 395. (d) Casado, A. L.; Espinet, P. *Organometallics* **1998**, *17*, 954. (e) Kayser, B.; Missling, C.; Knizek, J.; Noeth, H.; Beck, W. *Eur. J. Inorg. Chem.* **1998**, *3*, 375. (f) Guillevic, M.-A.; Rocaboy, C.; Arif, A. M.; Horvath, I. T.; Gladysz, J. A. *Organometallics* **1998**, *17*, 707. (g) Edelbach, B. L.; Lachicotte, R. J.; Jones, W. D. *J. Am. Chem. Soc.* **1998**, *120*, 2843. (h) Crabtree, R. H. *Chem. Rev.* **1995**, *95*, 987. (i) Grushin, V. V.; Alper, H. *Chem. Rev.* **1994**, *94*, 1047. (j) Ellis, P. R.; Pearson, J. M.; Haynes, A.; Adams, H.; Bailey, N. A.; Maitlis, P. M. *Organometallics* **1994**, *13*, 3215. (k) Wright, M. W.; Smalley, T. L.; Welker, M. E.; Rheingold, A. L. *J. Am. Chem. Soc.* **1994**, *116*, 6777. (l) Sakakaurka, T.; Sodeyama, T.; Sasaki, K.; Wada, K.; Tanaka, M. *J. Am. Chem. Soc.* **1990**, *112*, 7221. (m) Casalnuovo, A. L.; Calabrese, J. C.; Milstein, D. *J. Am. Chem. Soc.* **1988**, *110*, 6738. (n) Janowics, A. H.; Bergman, R. G. *J. Am. Chem. Soc.* **1983**, *105*, 3929. (o) Jones, W. D.; Feher, F. J. *J. Am. Chem. Soc.* **1982**, *104*, 4240. (p) Hickey, C. E.; Maitlis, P. M. *J. Chem. Soc., Chem. Commun.* **1984**, 1609. (q) Forster, D. *Adv. Organomet. Chem.* **1979**, *17*, 255. (r) Forster, D. *J. Am. Chem. Soc.* **1975**, *97*, 951.

(3) (a) Eller, K.; Schwarz, H. *Chem. Rev.* **1991**, *91*, 1121. (b) Armentrout, P. B.; Beauchamp, J. L. *Acc. Chem. Res.* **1989**, *22*, 315.

(4) Experimental studies on reactions of ionic metal atoms and complexes in the gas phase: (a) Brönstrup, M.; Schröder, D.; Schwarz, H.

Organometallics **1999**, *18*, 1939. (b) Aschi, M.; Brönstrup, M.; Diefenbach, M.; Harvey, J. N.; Schröder, D.; Schwarz, H. *Angew. Chem.* **1998**, *110*, 858. (c) Freiser, B. S. *J. Mass Spectrom.* **1996**, *31*, 703. (d) van Koppen, P. A. M.; Kemper, P. R.; Bushnell, J. E.; Bowers, M. T. *J. Am. Chem. Soc.* **1995**, *117*, 2098. (e) Wesendrup, R.; Schröder, D.; Schwarz, H. *Angew. Chem.* **1994**, *105*, 1232. (f) Chen, Y.-M.; Clemmer, D. E.; Armentrout, P. B. *J. Am. Chem. Soc.* **1994**, *116*, 7815. (g) van den Berg, K. J.; Ingemann, S.; Nibbering, N. M. M.; Gregor, I. K. *Rapid. Commun. Mass Spectrom.* **1993**, *7*, 769. (h) Chowdhury, A. K.; Wilkins, C. L. *J. Am. Chem. Soc.* **1987**, *109*, 5336. (i) Weil, D. A.; Wilkins, C. L. *J. Am. Chem. Soc.* **1985**, *107*, 7316. (j) Jones, R. W.; Staley, R. H. *J. Phys. Chem.* **1982**, *86*, 1669. (k) Jones, R. W., Staley, R. H. *J. Am. Chem. Soc.* **1980**, *102*, 3794.

(5) Combined experimental and theoretical studies on reactions of ionic metal atoms and complexes in the gas phase: (a) Yi, S. S.; Reichert, E. L.; Holthausen, M. C.; Koch, W.; Weisshaar, J. C. *Chem. Eur. J.* **2000**, *6*, 2232. (b) Blomberg, M.; Yi, S. S.; Noll, R. J.; Weisshaar, J. C. *J. Phys. Chem. A* **1999**, *103*, 7254. (c) Diefenbach, M.; Brönstrup, M.; Aschi, M.; Schröder, D.; Schwarz, H. *J. Am. Chem. Soc.* **1999**, *121*, 10614. (d) Schwarz, J.; Schröder, D.; Schwarz, H.; Heinemann, C.; Hrusák, J. *Helv. Chim. Acta* **1996**, *79*, 1110.

(6) Experimental studies on reactions of neutral metal atoms in the gas phase: (a) Wen Y.; Porembski, M.; Ferrett, T. A.; Weisshaar, J. C. *J. Phys. Chem. A* **1998**, *102*, 8362. (b) Wen, Y.; Yethiraj, A.; Weisshaar, J. C. *J. Chem. Phys.* **1997**, *106*, 5509. (c) Carroll, J. J.; Weisshaar, J. C. *J. Phys. Chem.* **1996**, *100*, 12355. (d) Chertihin, G. V.; Andrews, L. *J. Am. Chem. Soc.* **1994**, *116*, 8322. (e) Carroll, J. J.; Haug, K. L.; Weisshaar, J. C. *J. Am. Chem. Soc*. **1993**, *115*, 6962. (f) Carroll, J. J.; Weisshaar, J. C. *J. Am. Chem. Soc.* **1993**, *115*, 800. (g) Ritter, D.; Carroll, J. J.; Weisshaar, J. C. *J. Phys. Chem.* **1992**, *96*, *10636*. (h) Mitchell, S. A.; Hackett, P. A. *J. Chem. Phys.* **1990**, *93*, 7822. (i) Ritter, D.; Weisshaar, J. C. *J. Am. Chem. Soc.* **1990**, *112*, 6425. (j) Fayet, P.; Kaldor, A.; Cox, D. M. *J. Chem. Phys.* **1990**, *92*, 254.

(7) Combined experimental and theoretical studies on reactions of neutral metal atoms in the gas phase: (a) Porembski, M.; Weisshaar, J. C. *J. Phys. Chem. A* **2000**, *104*, 1524. (b) Carroll, J. J.; Haug, K. L.; Weisshaar, J. C.; Blomberg, M. R. A.; Siegbahn, P. E. M.; Svensson, M. *J. Phys. Chem.* **1995**, *99*, 13955. (c) Carroll, J. J.; Weisshaar, J. C.; Siegbahn, P. E. M.; Wittborn, A. M. C.; Blomberg, M. R. A. *J. Phys. Chem.* **1995**, *99*, 14388. (d) Mitchell, S.; Blitz, M. A.; Siegbahn, P. E. M.; Svenson, M. *J. Chem. Phys.* **1994**, *100*, 423. (e) Weisshaar, J. C. *Acc. Chem. Res.* **1993**, *26*, 213.

(8) Theoretical studies on reactions of metal complexes: (a) Dedieu, A. *Chem. Rev.* **2000**, *100*, 543. (b) Torrent, M.; Solà, M.; Frenking, G. *Chem. Rev.* **2000**, *100*, 439. (c) Griffin, T. R.; Cook, D. B.; Haynes, A.; Pearson, J. M.; Monti, D.; Morris, G. E. *J. Am. Chem. Soc.* **1996**, *118*, 3029. (d) Aullón, G.; Alvarez, S. *Inorg. Chem.* **1996**, *35*, 3137. (e) Ziegler, T. *Chem. Rev.* **1991**, *91*, 651. (f) Koga, N.; Morokuma, K. *Chem. Rev.* **1991**, *91*, 823. (g) Bickelhaupt, F. M.; Baerends, E. J.; Ravenek, W. *Inorg. Chem.* **1990**, *29*, 350.

(9) See also, for example: (a) Lamprecht, D.; Lamprecht, G. J. *J. Comput. Chem.* **2000**, *21*, 692. (b) Minaev, B.; Agren, H. *Int. J. Quantum Chem.* **1999**, *72*, 581. (c) Su, M.-D.; Chu, S.-Y. *J. Am. Chem. Soc*. **1999**, *121*, 1045. (d) Su, M.-D-; Chu, S.-Y. *Inorg. Chem.* **1998**, *37*, 3400. (e) Su, M.-D-; Chu, S.-Y. *Chem. Phys. Lett.* **1998**, *282*, 25. (f) Albert, K.; Gisdakis, P.; Rösch, N. *Organometallics* **1998**, *17*, 1608. (g) Sakaki, S.; Biswas, B.: Sugimoto, M. *Organometallics* **1998**, *17*, 1278. (h) Hill, G. S.; Puddephatt, R. J. *Organometallics* **1998**, *17*, 1478. (i) Sakaki, S.; Ogawa, M.; Kinoshita, M. *J. Phys. Chem.* **1995**, *99*, 9933. (j) Irikura, K. K.; Goddard, W. A., III. *J. Am. Chem. Soc.* **1994**, *116*, 8733. (k) Perry, J. K.; Goddard, W. A., III. *J. Am. Chem. Soc.* **1994**, *116*, 5013. (l) Sellers, H. *J. Comput. Chem.* **1990**, *11*, 754. (m) Rosi, M.; Bauschlinger, C. W., Jr.; Langhoff, S. R.; Partidge, H. *J. Phys. Chem.* **1990**, *94*, 8656. (n) Ziegler, T.; Tschinke, V.; Fan, L.; Becke, A. D. *J. Am. Chem. Soc.* **1989**, *111*, 9177. (o) Low, J. J.; Goddard, W. A., III. *J. Am. Chem. Soc.* **1986**, *108*, 6115.

(10) (a) Bickelhaupt, F. M. *J. Comput. Chem.* **1999**, *20*, 114. (b) Bickelhaupt, F. M.; Ziegler, T.; von Ragué Schleyer, P. *Organometallics* **1995**, *14*, 2288.

(11) Theoretical studies on reactions of neutral metal atoms: (a) Maseras, F.; Lledós, A.; Clot, E.; Eisenstein, O. *Chem. Rev.* **2000**, *100*, 601. (b) Cui, Q.; Musaev, D. G.; Morokuma, K. *J. Chem. Phys.* **1998**, *108*, 8418. (c) Wittborn, A. M. C.; Costas, M.; Blomberg, M. R. A.; Siegbahn, P. E. M. *J. Chem. Phys.* **1997**, *107*, 4318. (d) Siegbahn, P. E. M. *J. Am. Chem. Soc.* **1994**, *116*, 7722. (e) Siegbahn, P. E. M. *Organometallics* **1994**, *13*, 2833. (f) Perry, J. K.; Ohanessian, G.; Goddard, W. A., III. *Organometallics* **1994**, *13*, 1870. (g) Blomberg, M. R. A.; Siegbahn, P. E. M.; Svensson, M. *Inorg. Chem.* **1993**, *32*, 4218. (h) Siegbahn, P. E. M.; Blomberg, M. R. A.; Svensson, M. *J. Phys. Chem*. **1993**, *97*, 2564. (i) Siegbahn, P. E. M.; Blomberg, M. R. A.; Svensson, M. *J. Am. Chem. Soc.* **1993**, *115*, 1952. (j) Siegbahn, P. E. M.; Blomberg, M. R. A.; Svensson, M. *J. Am. Chem. Soc.* **1993**, *115*, 4191. (k) Siegbahn, P. E. M.; Blomberg, M. R. A. *J. Am. Chem. Soc.* **1992**, *114*, 10548. (l) Blomberg, M. R. A.; Siegbahn, P. E. M.; Svensson, M. *J. Am. Chem. Soc.* **1992**, *114*, 6095. (m) Svensson, M.; Blomberg, M. R. A.; Siegbahn, P. E. M. *J. Am. Chem. Soc.* **1991**, *113*, 7076. (n) Novaro, O.; Jarque, C. *Theor. Chim. Acta* **1991**, *80*, 19. (o) Blomberg, M. R. A.; Siegbahn, P. E. M.; Nagashima, U.; Wennerberg, J. *J. Am. Chem. Soc.* **1991**, *113*, 424. (p) Carter, E. A.; Goddard, W. A., III. *J. Phys. Chem.* **1988**, *92*, 5679. (q) Nakatsuji, H.; Hada, M.; Yonezawa, T. *J. Am. Chem. Soc.* **1987**, *109*, 1902. (r) Low, J. J.; Goddard, W. A., III. *Organometallics* **1986**, *5*, 609. (s) Koga, N.; Obara, S.; Kitaura, K.; Morokuma, K. *J. Am. Chem. Soc*. **1985**, *107*, 7109. (t) Low, J. J.; Goddard, W. A., III. *J. Am. Chem. Soc.* **1984**, *106*, 8321.

(12) Relativistic effects: (a) Moss, R. E. *Advanced Molecular Quantum Mechanics*; Chapman and Hall: London, 1973. (b) Pyykkö, P. *Chem. Rev.* **1988**, *88*, 563.

(13) (a) Basile, A.; Fasson, S.; Vitulli, G.; Drioli, E. *Stud. Surf. Sci. Catal.* **1998**, *119*, 453. (b) Malleron, J.-L.; Fiaud, J.-C.; Legros, J.-Y. *Handbook of Palladium Catalyzed Organic Reactions*; Academic Press: 1997. (c) Cornils, R.; Herrmann, W. A. *Applied Homogeneous Catalysis with Organometallic Compounds*; VCH: Weinheim, 1996; Vol. 1, p 394.

(14) Diefenbach, A.; Bickelhaupt, F. M. *J. Chem. Phys.* **2001**, *115*, 4030.

(15) Density functional theory (DFT): (a) Dreizler, R. M.; Gross, E. K. U. *Density Functional Theory. An approach to the Quantum Many-Body Problem*; Springer: Berlin, 1990. (b) Parr, R. G.; Yang, W. *Density-Functional Theory of Atoms and Molecules*; Oxford University Press: New York, 1989.

(16) Kohn−Sham MO model in DFT: (a) Bickelhaupt, F. M.; Baerends, E. J. In *Reviews in Computational Chemistry*; Lipkowitz, K. B., Boyd., D. B., Eds.; Wiley-VCH: New York, 2000; Vol. 15, Chapter 1. (b) Baerends, E. J.; Gritsenko, O. V. *J. Phys. Chem. A* **1997**, *101*, 5383.

(17) Amsterdam density functional (ADF) program: (a) te Velde, G.; Bickelhaupt, F. M.; Baerends, E. J.; van Gisbergen, S. J. A.; Fonseca Guerra, C.; Snijders, J. G.; Ziegler, T. *J. Comput. Chem.* **2001**, *22*, 931. (b) Baerends, E. J.; Ellis, D. E.; Ros, P. *Chem. Phys.* **1973**, *2*, 41. (c) Baerends, E. J.; Ros, P. *Chem. Phys.* **1975**, *8*, 412. (d) Baerends, E. J.; Ros, P. *Int. J. Quantum Chem., Quantum Chem. Symp.* **1978**, *S12*, 169. (e) Fonseca Guerra, C.; Snijders, J. G.; te Velde, G.; Baerends, E. J. *Theor. Chem. Acc.* **1998**, *99*, 391. (f) Boerrigter, P. M.; te Velde, G.; Baerends, E. J. *Int. J. Quantum Chem.* **1988**, *33*, 87. (g) te Velde, G.; Baerends, E. J. *J. Comput. Phys.* **1992**, *99*, 84. (h) Snijders, J. G.; Baerends, E. J.; Vernooijs, P. *At. Nucl. Data Tables* **1982**, *26*, 483. (i) Krijn, J.; Baerends, E. J. *Fit-Functions in the HFS-Method, Internal Report* (in Dutch); Vrije Universiteit: Amsterdam, 1984. (j) Slater, J. C. *Quantum Theory of Molecules and Solids*; McGraw-Hill: New York, 1974; Vol. 4. (k) Becke, A. D. *J. Chem. Phys.* 1986, *84*, 4524. (l) Becke, A. *Phys. Rev. A* **1988**, *38*, 3098. (m) Vosko, S. H.; Wilk, L.; Nusair, M. *Can. J. Phys.* **1980**, *58*, 1200. (n) Perdew, J. P. *Phys. Rev. B* **1986**, *33*, 8822 (Erratum: *Phys. Rev. B* **1986**, *34*, 7406). (o) Fan, L.; Ziegler, T. *J. Chem. Phys.* **1991**, *94*, 6057. (p) Versluis, L.; Ziegler, T. *J. Chem. Phys.* **1988**, *88*, 322. (q) Fan, L.; Versluis, L.; Ziegler, T.; Baerends, E. J.; Ravenek, W. *Int. J. Quantum. Chem., Quantum. Chem. Symp.* **1988**, *S22*, 173. (r) Fan, L.; Ziegler, T. *J. Chem. Phys.* **1990**, *92*, 3645. (s) Banerjee, A.; Adams, N.; Simons, J.; Shepard, R. *J. Phys. Chem.* **1985**, *89*, 52. (t) Baker, J. *J. Comput. Chem.* **1986**, *7*, 385.

(18) ZORA approach: (a) Chang, C.; Pelissier, M.; Durand, P. *Phys. Scr.* **1986**, *34*, 394. (b) van Lenthe, E.; Baerends, E. J.; Snijders, J. G. *J. Chem. Phys.* **1993**, *99*, 4597. (c) van Lenthe, E.; Baerends, E. J.; Snijders, J. G. *J. Chem. Phys.* **1994**, *101*, 9783. (d) van Lenthe, E.; van Leeuwen, R.; Baerends, E. J.; Snijders, J. G. *Int. J. Quantum Chem.* **1996**, *57*, 281.

(19) Atkins, P. W. *Physical Chemistry*; Oxford University Press: Oxford, 1998.

(20) A negative activation energy does not imply the complete absence of any barrier. The reaction is still hampered by a statistical or entropic bottleneck that is associated with the decrease in the number of available quantum states (e.g., of translation, rotation, and vibration) as one goes from the separate, unbound reactants to the tightly bound transition state.

(21) Bond energy decomposition: (a) Ziegler, T.; Rauk, A. *Inorg. Chem.* **1979**, *18*, 1558. (b) Ziegler, T.; Rauk, A. *Inorg. Chem.* **1979**, *18*, 1755. (c) Ziegler, T.; Rauk, A. *Inorg. Chem.* **1977**, *16*, 1. (d) Bickelhaupt, F. M.; Nibbering, N. M. M.; van Wezenbeek, E. M.; Baerends, E. J. *J. Phys. Chem.* **1992**, *96*, 4864.

(22) In the solution phase, the extreme endothermicity associated with charge separation in the straight S_N2 reactions that are considered here in the gas phase will be significantly tempered (and possibly turned into exothermicity) because the ionic products are much more strongly stabilized by solvation than the neutral reactants. Likewise, the transition state for the S_N2/Cl-ra reaction, in which palladium and chlorine are partially positively and negatively charged, respectively, will be stabilized relative to the reactants, leading to a lowering of the barrier; see, for example, ref 10b.

(23) We anticipate that introducing ligands into the catalytically active transition metal system brings into play the phenomenon of ligand reorganization as an additional important factor that affects the activation strain of the reaction.

(24) Holleman, A. F.; Wiberg, N. *Lehrbuch der Anorganischen Chemie*; de Gruyter: Berlin, 1985.

(25) Albright, T. A.; Burdett, J. K.; Whangbo, M.-H. *Orbital Interactions in Chemistry*; Wiley-Interscience: New York, 1985.